www.springer.com/41230
https://doi.org/10.1007/s41230-025-4285-9
Research & Development
Vol. 23 No. 1 January 2026
CHINA FOUNDRY

On AlN_P/Mg-Zn-Cu cast composites with low expansion and high thermal conductivity

***Shu-sen Wu, Lu Chen, Shu-lin Lü, Wei Guo, and Jian-yu Li**

State Key Lab of Materials Processing and Die & Mould Technology, School of Materials Science and Engineering, Huazhong University of Science and Technology, Wuhan 430074, China

Abstract: There is an urgent need to develop magnesium-matrix materials that exhibit both high thermal conductivity and low thermal expansion to ensure compatibility with chips. This study aims to develop a Mg-Zn-Cu alloy with high thermal conductivity. Furthermore, it explores the preparation of AlN_P/Mg-Zn-Cu composites featuring low coefficients of thermal expansion. The stir casting method was utilized to fabricate the composites and an investigation was conducted to examine their microstructure and thermal properties. Results indicate that the addition of AlN_P reduces the thermal expansion coefficient while maintaining relatively high thermal conductivity. Specifically, the AlN_P/Mg-0.5Zn-0.5Cu composite with 30wt.% AlN_P achieves a thermal conductivity of 132.7 $W·m^{-1}·K^{-1}$ and a thermal expansion coefficient of $18.5×10^{-6}$ K^{-1}, rendering it suitable for electronic packaging applications where thermal management is critical.

Keywords: thermal expansion; thermal conductivity; magnesium-matrix composites; Mg-Zn-Cu alloy

CLC numbers: TG146.22 **Document code:** A **Article ID:** 1672-6421(2026)01-101-07

1 Introduction

The evolution of integrated circuits is characterized by miniaturization, high integration, and increased power consumption, with chip power density reaching 10^4 $W·cm^{-2}$ [1]. High power density signifies substantial heat generation during chip operation, leading to elevated operating temperatures that are challenging to dissipate efficiently. Studies indicate that for every 10 °C increase in chip temperature, the lifespan is halved, and high-temperature-induced failures account for 55% of all failure modes[2]. Elevated operating temperatures in chips exacerbate thermal stress, a primary mechanism of high-temperature failure. Thermal stress results from the mismatch in thermal expansion coefficients (CTE) between semiconductor and packaging materials. Therefore, mitigating thermal stress during chip operation is crucial for enhancing reliability and stability.

Thermal stress can be alleviated by lowering the operating temperature of the chip and reducing the CTE of packaging materials. Utilizing packaging materials with high thermal conductivity and low CTE effectively addresses this challenge. Chip packaging serves multiple critical functions, including providing electrical connections, mechanical support, physical protection, and efficient heat dissipation. Packaging materials with high thermal conductivity facilitate efficient heat transfer from the chip's interior to its exterior, thereby reducing operating temperatures. Currently, packaging materials primarily consist of plastics, ceramics, and metals, with ceramics and metals demonstrating superior thermal conductivity[3]. Additionally, ceramics exhibit low thermal expansion, while metals provide good processability. Consequently, in recent years, metal matrix composites reinforced with ceramic particles have seen increased application in the packaging field[4].

Magnesium (Mg), the lightest structural material available, exhibits a high thermal conductivity of 156 $W·m^{-1}·K^{-1}$ at room temperature, which is significantly higher than that of plastic packaging, and is second only to common metals like copper (Cu) and aluminum (Al)[5]. Furthermore, magnesium offers excellent electromagnetic shielding and vibration damping properties, which prevent electromagnetic interference in high-frequency integrated circuits and enhance the vibration reliability of the packaging, making it an

***Shu-sen Wu**

Male, Ph. D., Professor. His research interests mainly focus on Al alloys, Mg alloys and their composites.

E-mail: ssw636@hust.edu.cn

Received: 2024-12-18; Revised: 2025-02-18; Accepted: 2025-02-24

ideal metal for packaging applications. However, magnesium has a relatively high average CTE of 26.0×10^{-6} K^{-1} between 20–100 °C, which limits its direct use as a packaging material[6]. Magnesium matrix composites reinforced with high-thermal conductivity ceramic particles retain the benefits of magnesium while reducing its CTE, making them promising candidates for metal matrix packaging materials.

Currently, the reinforcement phase in metal-matrix packaging materials predominantly comprises diamond particles. To achieve high thermal conductivity, large diamond particles with sizes exceeding 100 μm are typically employed[7,8]. This approach presents two significant drawbacks: first, the cost of diamond raw materials is substantially high, ranging from 50 to 200 times that of the matrix alloy. Second, the use of large diamond particles complicates the processing of metal matrix composites, thereby restricting the available forming and processing methods. Aluminum nitride (AlN), an emerging ceramic material, exhibits a high thermal conductivity of 320 $W\cdot m^{-1}\cdot K^{-1}$ and a low CTE of 4.5×10^{-6} K^{-1}, with a cost that is only 10% to 40% of that of diamond[9,10]. Consequently, utilizing aluminum nitride particles (AlN_p) as a novel reinforcement phase can significantly reduce the cost of metal matrix packaging materials and broaden their range of applications. This study utilized the stir casting method to fabricate AlN_p/Mg-Zn-Cu composites and investigated their microstructures and thermal properties. The aim is to explore the potential applications of these composites in the field of chip packaging.

2 Experimental procedure

Pure magnesium ingot (99.5%), zinc ingot (99.9%), and copper ingot (99.95%) were melted in a resistance furnace to synthesis Mg-*x*Zn-*x*Cu (*x*=0.5, 1, 3, 5, in wt.%) alloys and these alloys were denoted as ZC00, ZC11, ZC33, and ZC55, respectively. Following a preliminary investigation, a ZC*xx* alloy would be selected as the matrix alloy to prepare the AlN_p/ZC*xx* composite. A cylindrical steel mold, preheated to 200 °C, with dimensions of Φ35 mm×120 mm, was employed in this study. AlN_p particles, averaging 10 μm in size, were incorporated into the melt using a semi-solid stirring technique to produce AlN_p/Mg-Zn-Cu composites with 10wt.%, 20wt.%, and 30wt.% AlN_p concentrations, as described in Ref. [11]. After synthesis, the melt was rapidly poured into the preheated mold mentioned above, squeezed, and solidified under a squeezing pressure of 50 MPa. Metallographic and SEM analysis methods are detailed in Ref. [12].

The process for calculating thermal conductivity is as follows:

$$\lambda=\alpha\cdot C\cdot\rho \quad (1)$$

where the thermal diffusivity (α) was measured using an LFA-427 laser flash apparatus on samples with dimensions of Φ12.7 mm×3 mm, and the measurements were repeated five times for each temperature condition. The specific heat capacity (C) of the composite was estimated using the Neumann-Kopp rule, which calculating it as the mass-weighted sum of the specific heats of both the matrix and reinforcement materials, as expressed by the following equation:

$$C=\sum C_i w_i \quad (2)$$

where, C_i and w_i denote the specific heat and mass percentage of each component, respectively. The room temperature density (ρ) of the material was measured using the Archimedes drainage method. The measurement was repeated five times for each sample, and the average, excluding the highest and lowest values, was taken as the final result. The thermal expansion coefficient was measured using a NETZSCH DIL402 thermal expansion meter across a temperature range of 20–300 °C. Tensile tests were conducted using a C45.105EY multi-material mechanical properties testing machine from the MTS Systems (China) Co., Ltd., with a tensile rate of 1 $mm\cdot min^{-1}$. At least five tests were repeated for each material, and the average value was used as the final result.

3 Results and discussion

3.1 Composition design of Mg-Zn-Cu matrix alloys

In previous research, our team developed a Mg-*x*Zn-*x*Cu (*x*=1, 3, 5, in wt.%) alloy system, noted for its high thermal conductivity, making it suitable as the matrix alloy for AlN_p reinforced composites[12]. In this study, the concentrations of Cu and Zn were further reduced to 0.5wt.%, creating an alloy referred to as ZC00. Due to the poor wettability between AlN_p and the magnesium melt, semi-solid stirring technology was employed to effectively introduce AlN_p into the matrix[13]. The presence of Cu in the alloy system facilitates semi-solid stirring because the Mg-Cu system has a wide liquid-solid phase range, and the solubility of Cu in Mg is very low, as shown in the Mg-Cu phase diagram in Fig. 1, which was generated using Thermo-Calc thermodynamic calculation software. Therefore, reducing the alloy content to 0.5wt.% is beneficial for the composite preparation process.

The as-cast alloys consist of α-Mg, which appears as dark regions, and a secondary phase, visible as light regions, distributed along the grain boundaries, as illustrated in

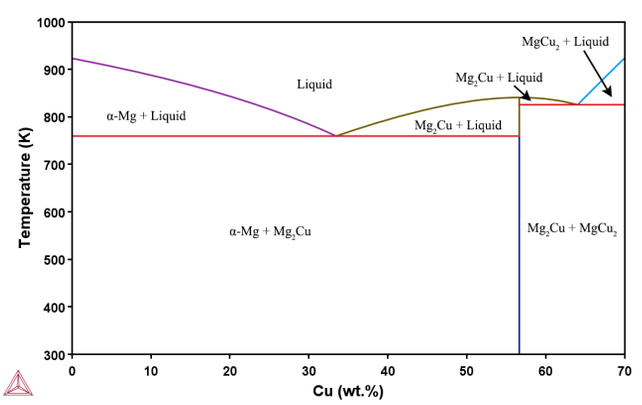

Fig. 1: Mg-Cu phase diagram

Fig. 2. Previous studies have identified this secondary phase as the MgCuZn ternary phase[12]. During solidification, the MgCuZn phase precipitates eutectically. As the content of alloying elements increases, the amount of the MgCuZn phase increases, leading to a reduction in grain size. This grain refinement occurs due to the accumulation of solute atoms at the solidification front, which causes compositional undercooling.

Subsequently, the thermal physical properties of the as-cast ZC00 alloy were compared with those of Mg-*x*Zn-*x*Cu (*x*=1, 3, 5, in wt.%) alloys, as illustrated in Fig. 3. As the content of alloying elements increases, the thermal conductivity of the four alloys decreases, while the CTE increases. The ZC00 alloy exhibits the highest room temperature thermal conductivity (152.1 $W \cdot m^{-1} \cdot K^{-1}$) and the lowest average CTE (24.5×10^{-6} K^{-1}, 20–100 °C). The ZC00 alloy's high thermal conductivity is attributed to its minimal lattice distortion. The degree of lattice distortion in magnesium alloys can be assessed by the ratio of the lattice constants along the *c*-axis and *a*-axis (*c*/*a* ratio). The closer this ratio is to the theoretical value (1.6235), the less the lattice distortion. Figure 4 illustrates the variation in the lattice axis ratio for the four different alloys. As the content of alloying elements increases, the *c*/*a* ratio increases from 1.6242 to 1.6299. Consequently, the ZC00 alloy exhibits the lowest lattice distortion, resulting in the highest thermal conductivity. Overall, the ZC00 alloy is more suitable as the matrix alloy for AlN_p-reinforced magnesium matrix composites. Subsequent research will focus on the thermal physical properties of AlN_p/ZC00 composites.

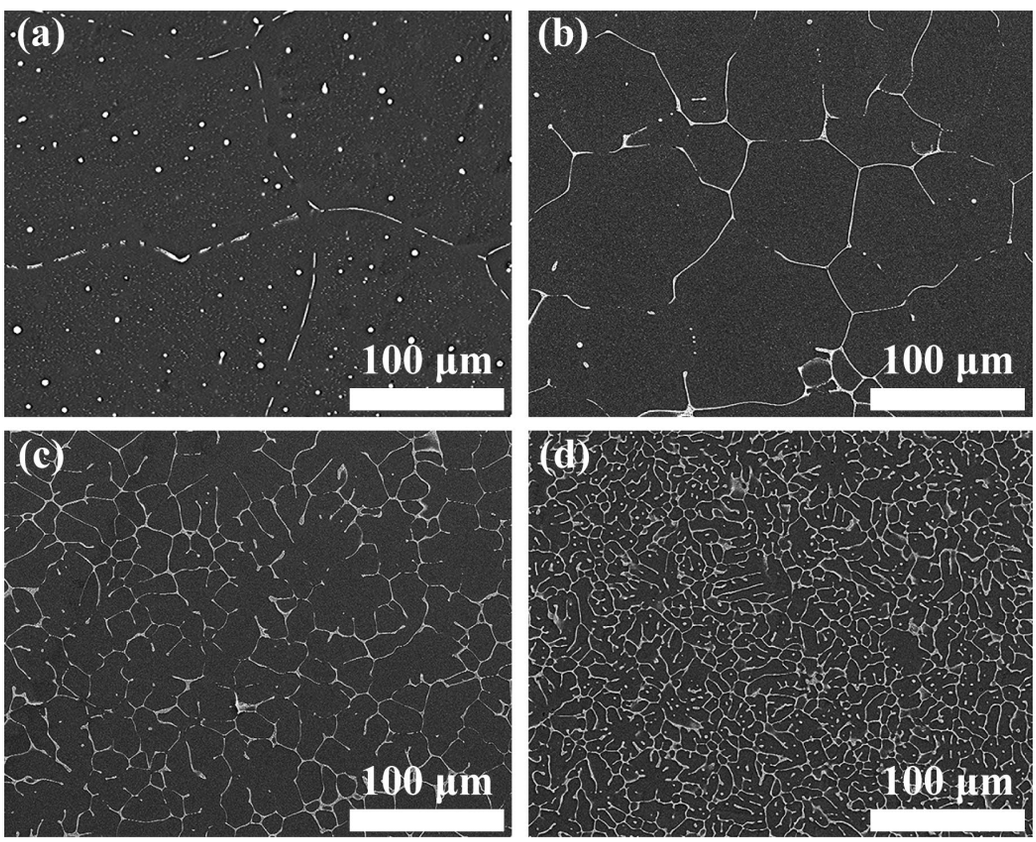

Fig. 2: SEM images of typical microstructure of Mg-Zn-Cu alloys: (a) ZC00; (b) ZC11; (c) ZC33; (d) ZC55

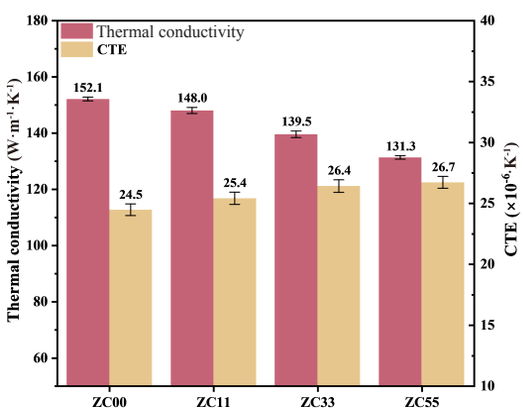

Fig. 3: Thermal physical properties of Mg-*x*Zn-*x*Cu (*x*=0.5, 1, 3, 5, in wt.%)

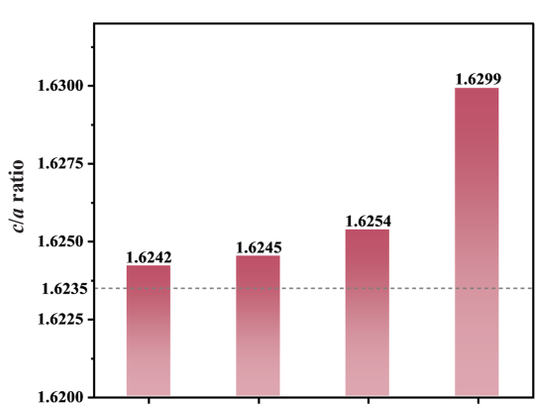

Fig. 4: *c*/*a* axis ratio of Mg-*x*Zn-*x*Cu (*x*=0.5, 1, 3, 5, in wt.%)

3.2 Microstructure and properties of AlN_P/ZC00 composites

Figure 5 shows the microstructure of AlN_P/ZC00 composites, featuring different contents of AlN_P particles, with an average particle size of 10 μm. As the AlN_P content increases, their distribution transitions from an initially uneven arrangement along the grain boundaries to a more uniform distribution throughout the entire matrix, with more AlN_P particles entering the interior of the α-Mg matrix. However, when the mass fraction of AlN_P exceeds 30%, significant solidification cracks appear within the composites. These cracks occur due to that the high content of AlN_P particles impedes the shrinkage of the matrix during solidification. Therefore, in this study, the maximum particle mass fraction of AlN_P in AlN_P/ZC00 composites is limited to 30%.

Figure 6 illustrates the response of the thermal conductivity of AlN_P/ZC00 composites to varying AlN_P content. As the AlN_P content increases, both the thermal diffusivity and thermal conductivity of the composites significantly decrease. When the mass fraction of AlN_P reaches 30%, the room temperature thermal diffusivity of the composites drops to 69.0 $mm^2 \cdot s^{-1}$, and the thermal conductivity decreases to 132.7 $W \cdot m^{-1} \cdot K^{-1}$, which remains higher than that of most magnesium alloys. Thermal conductivity indicates a material's capacity to transfer heat, whereas thermal diffusivity reflects its ability to uniformly distribute temperature internally. Thermal diffusivity is measured directly using the laser flash method, offering a more intuitive assessment of the material's heat dissipation capability. The steepness of thermal diffusivity is associated with the

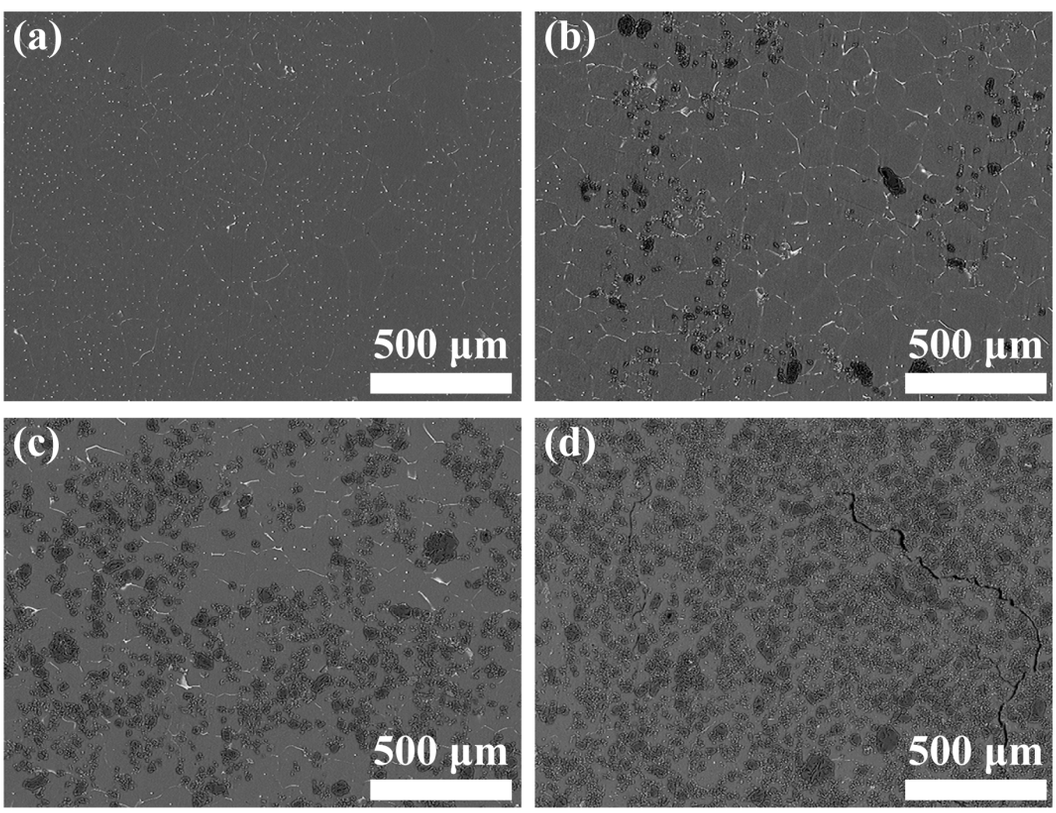

Fig. 5: BSE images of AlN_P/ZC00 composites with different particle contents: (a) ZC00; (b) 10wt.% AlN_P/ZC00; (c) 20wt.% AlN_P/ZC00; (d) 30wt.% AlN_P/ZC00

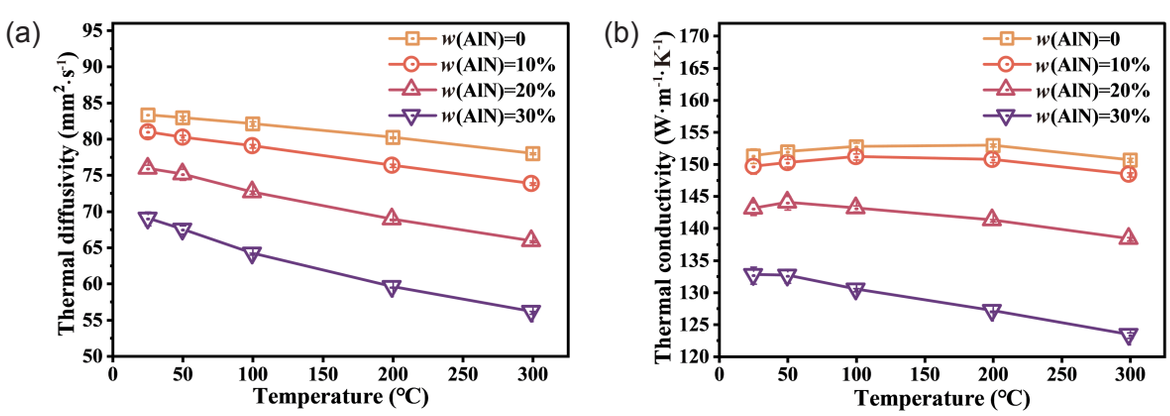

Fig. 6: Thermal diffusivity curve (a) and thermal conductivity curve (b) of AlN_P/ZC00 composites with different particle contents

scattering mechanism of carriers within the material; greater steepness indicates a higher probability of carrier scattering. As the AlN_P content increases, both the thermal diffusivity and its steepness in the four materials decrease. This suggests that AlN_P introduces additional electron and phonon scattering in the composites, thereby reducing its thermal conductivity efficiency.

The decrease in the thermal conductivity of the composites indicates that the effective thermal conductivity of AlN_P is lower than that of the matrix alloy. This reduction is primarily due to the poor wettability between AlN_P and Mg, which results in additional contact thermal resistance at the AlN/Mg interface, thus limiting the ability of AlN_P to exert its high thermal conductivity effect. Comparing the peak thermal conductivity temperatures among the four curves in Fig. 6, it can be seen as the AlN_P content increases, the temperature corresponding to the peak thermal conductivity gradually shifts to lower values. This shift occurs because the thermal carriers in AlN_P are phonons, and at high temperatures, the anharmonic vibrations of phonons are enhanced, leading to a decrease in the thermal conductivity of AlN_P with increasing temperature[14]. The higher the AlN_P content in the composites, the more pronounced the overall decline in thermal conductivity, causing the peak temperature to shift leftward, and thus the thermal conductivity curve to enter the declining phase earlier. Additionally, cracks and pores in the composites with a high particle content introduce gas or vacuum with low thermal conductivity, further weakening the composite's thermal conductivity. The experimental results indicate that AlN_P reduces the thermal conductivity of AlN_P/ZC00 composites, and this reduction effect becomes more pronounced as the AlN_P content increases.

Although AlN_P does not improve thermal conductivity of the composites, it significantly affects their thermal dimensional stability. Figure 7 illustrates the response of the average CTE of AlN_P/ZC00 composites, referenced at 20 °C, across different temperatures and AlN_P content levels. Generally, the CTE of all four materials increases with rising temperature, primarily due to the enhanced anharmonic vibrations of magnesium atoms at elevated temperatures. This study focuses on the average CTE in the 20–100 °C range, which corresponds to the operating temperature range of most electronic devices. Unless otherwise specified, the CTE mentioned refers to the average value within this range. The average CTE of the matrix alloy ZC00 is 24.5×10^{-6} K^{-1} at 20 °C, which is similar to that of pure magnesium due to the minimal addition of alloying elements. As shown in Fig. 7(b), the CTE of AlN_P/ZC00 composites gradually decreases as the AlN_P content increases. When the AlN_P content reaches a maximum of 30%, the CTE of the composites decreases to 18.5×10^{-6} K^{-1}, representing a reduction of 24.5% compared to the matrix alloy. In Fig. 7(b), the relationship between CTE and AlN_P volume fraction for the four materials is fitted. The predictions made by the Kerner model closely align with the experimental results, whereas the predictions of the rule of mixtures (ROM) model are significantly higher. The Kerner model expression comprehensively considers the effects of the volume fraction and modulus of the reinforcement. The expressions for the ROM [Eq. (4)] and Kerner [Eq. (5)] models are as follows[15, 16]:

$$\alpha_c = \alpha_m V_m + \alpha_p V_p \tag{4}$$

$$\alpha_c = \alpha_m V_m + \alpha_p V_p + V_m V_p (\alpha_p - \alpha_m) \frac{K_p - K_m}{V_m K_m + V_p K_p + \frac{3K_m K_p}{4G_m}} \tag{5}$$

where α_c, α_m, and α_p denote the CTEs of the composite, matrix, and reinforcement phase, respectively, while V_m and V_p denote the volume fractions of the matrix and reinforcement phase. K_m, G_m, and K_p correspond to the bulk modulus and shear modulus of the matrix, and bulk modulus of the reinforcement phase, respectively. It is clear that the ROM model consists of only the first two terms of the Kerner model essentially. The third term in the Kerner model accounts for the effect of the modulus, which increases with the modulus of the reinforcement phase. The bulk moduli of magnesium and AlN_P are 35 GPa and 210 GPa, respectively[17]. At 30% AlN_P content, this term contributes to an additional reduction in the CTE by 2.0×10^{-6} K^{-1}, accounting for 50% of the reduction predicted by the ROM model.

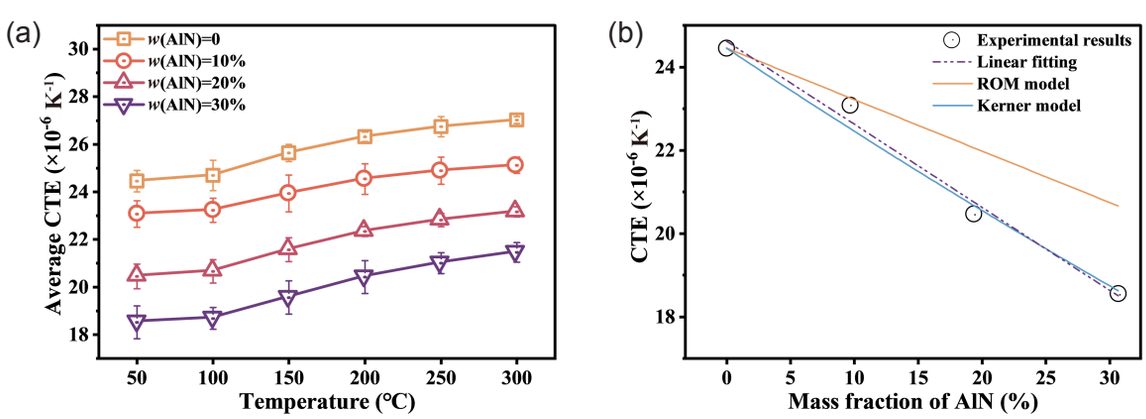

Fig. 7: CTE of AlN_P/ZC00 composites with different particle contents: (a) average CTE versus temperature curve; (b) average CTE versus AlN_P content

The mechanical properties of AlN_P/ZC00 composites were also investigated, as illustrated by the stress-strain curves of the four materials in Fig. 8. The addition of 10wt.% AlN_P enhances both the tensile strength and elongation of the composites. Among the four materials, the composite with 10wt.% AlN_P content exhibits the optimal mechanical properties. Specifically, it has a tensile strength of 174 MPa and an elongation of 14.2% in the as-cast state. These values represent a 16% increase in tensile strength and a 13% increase in elongation compared to the ZC00 matrix alloy, which has a tensile strength of 150 MPa and an elongation of 12.6%. Increasing the particle content beyond this level to 20wt.% or 30wt.% leads to a sharp decline in the composite's plasticity and strength. Figure 8 also indicates that the elastic modulus of the composite increases with AlN_P content, attributed to AlN_P's high elastic modulus. As previously noted, the bulk modulus of AlN_P is 210 GPa, effectively restricting the thermal expansion of the magnesium matrix. The elastic modulus of AlN_P is 330 GPa, which is seven times as that of the Mg matrix, thereby increasing the stiffness of the composites[18]. Introduction of an appropriate amount of AlN_P enhances the composite's mechanical and thermal expansion properties, although with a slight reduction in thermal conductivity. As observed in the microstructure shown in Fig. 5, a small amount of AlN_P refines the composite's grains, enhancing its plasticity. Further increasing the AlN_P content, over 10wt.%, impedes the feeding of the ZC00 melt during solidification, leading to solidification cracks and a sharp deterioration in the composite's mechanical properties.

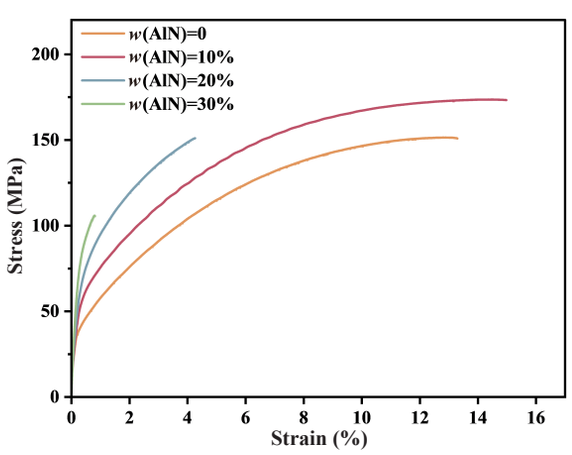

Fig. 8: Room temperature tensile curves of AlN_P/ZC00 composites

4 Conclusions

(1) Among the four Mg-*x*Zn-*x*Cu (*x*=0.5, 1, 3, 5, in wt.%) alloys, the ZC00 (*x*=0.5wt.%) alloy exhibits the highest thermal conductivity, reaching 153.0 $W \cdot m^{-1} \cdot K^{-1}$. The ZC00 alloy possesses the widest liquidus-solidus temperature range, making it suitable for the semi-solid preparation of composites. These properties render it the optimal matrix material for AlN_P-reinforced magnesium-based composites.

(2) As the AlN_P content in the AlN_P/ZC00 composites increases, both the thermal conductivity and the CTE decrease. When the mass fraction of AlN_P reaches 30%, the composites exhibit a relatively higher thermal conductivity of 132.7 $W \cdot m^{-1} \cdot K^{-1}$ and a lower CTE of 18.5×10^{-6} K^{-1}.

(3) The addition of 10wt.% AlN_P enhances both the tensile strength and elongation of the AlN_P/ZC00 composites. The 10wt.% AlN_P/ZC00 composite demonstrates the optimal overall mechanical properties among the four materials, with a tensile strength of 174 MPa and an elongation of 14.2% in as-cast state.

Acknowledgments

This work was financially supported by National Natural Science Foundation of China (No. 52175321) and the Fund of Key Laboratory of High Temperature Electromagnetic Materials and Structure of MOE (No. KB202505).

Conflict of interest

Prof. Shu-sen Wu is an EBM of *CHINA FOUNDRY*. He was not involved in the peer-review or handling of the manuscript. The authors have no other competing interests to disclose.

References

[1] He Z, Yan Y, Zhang Z. Thermal management and temperature uniformity enhancement of electronic devices by micro heat sinks: A review. Energy, 2021, 216: 119223. https://doi.org/10.1016/j.energy.2020.119223.

[2] Bailey C. Thermal management technologies for electronic packaging: Current capabilities and future challenges for modelling tools. 10th Electron. Packag. Technol. Conf. Singapore, Singapore: IEEE, 2008: 527–532. http://ieeexplore.ieee.org/document/4763487/. https://doi.org/10.1109/EPTC.2008.4763487.

[3] Moore A L, Shi L. Emerging challenges and materials for thermal management of electronics. Mater. Today, 2014, 17(4): 163–174. https://doi.org/10.1016/j.mattod.2014.04.003.

[4] Silvain J F, Heintz J M, Veillere A, et al. A review of processing of Cu/C base plate composites for interfacial control and improved properties. Int. J. Extreme Manuf., 2020, 2(1): 12002. https://doi.org/:10.1088/2631-7990/ab61c5.

[5] Abu-Eishah S I. Correlations for the thermal conductivity of metals as a function of temperature. Int. J. Thermophys., 2001, 22(6): 1855–1868. https://doi.org/10.1023/A:1013155404019.

[6] Zhang B, Li X, Li D. Assessment of thermal expansion coefficient for pure metals. Calphad, 2013, 43: 7–17. https://doi.org/10.1016/j.calphad.2013.08.006.

[7] Peng J, Zhang F, Zhou Y, et al. Fabrication of diamond/copper composite thin plate based on a single-layer close packed diamond particles network for heat dissipation. Chem. Eng. J., 2023, 476: 146666. https://doi.org/10.1016/j.cej.2023.146666.

[8] Xie Z, Guo H, Zhang X, et al. Tailoring the thermal and mechanical properties of diamond/Cu composites by interface regulation of Cr alloying. Diam. Relat. Mater., 2021, 114: 108309. https://doi.org/10.1016/j.diamond.2021.108309.

[9] Medraj M, Baik Y, Thompson W T, et al. Understanding AlN sintering through computational thermodynamics combined with experimental investigation. J. Mater. Process. Technol., 2005, 161(3): 415–422. https://doi.org/10.1016/j.jmatprotec.2004.05.031.
[10] Chen L, Lü S, Zhao D, et al. Progress in preparation of AlN-reinforced magnesium matrix composites: A review. China Foundry, 2024, 21(1): 1–10. https://doi.org/10.1007/s41230-023-3035-0.
[11] Chen L, Qin J, Li J Y, et al. Semi-solid casting of AlN reinforced Mg-matrix composites and their thermophysical properties. Solid State Phenom., 2023, 347: 91–96. https://doi.org/10.4028/p-2o4lMz.
[12] Chen L, Lü S, Guo W, et al. High thermal conductivity of highly alloyed Mg-Zn-Cu alloy and its mechanism. J. Alloys Compd., 2022, 918: 165614. https://doi.org/10.1016/j.jallcom.2022.165614.
[13] Shi W, Kobashi M, Choh T. Wettability of molten magnesium on carbon and AlN. J. Jpn. Inst. Met., 2000, 64(5): 335–338. https://doi.org/10.2320/JINSTMET1952.64.5-335.
[14] Cheng Z, Koh Y R, Mamun A, et al. Experimental observation of high intrinsic thermal conductivity of AlN. Phys. Rev. Mater., 2020, 4(4): 044602. https://doi.org/10.1103/PhysRevMaterials.4.044602.
[15] Yang Z, He X, Wang L, et al. Microstructure and thermal expansion behavior of diamond/SiC/(Si) composites fabricated by reactive vapor infiltration. J. Eur. Ceram. Soc., 2014, 34(5): 1139–1147. https://doi.org/10.1016/j.jeurceramsoc.2013.10.038.
[16] Li W, Nie K, Deng K, et al. Simultaneously improved modulus, thermal expansion coefficient and wear resistance of a Mg-6Zn-1Gd-0.3Ca matrix composite by adding high volume fraction SiC particles. J. Mater. Res. Technol., 2023, 26: 4282–4295. https://doi.org/10.1016/j.jmrt.2023.08.143.
[17] Iuga M, Steinle-Neumann G, Meinhardt J. Ab-initio simulation of elastic constants for some ceramic materials. Eur. Phys. J. B, 2007, 58(2): 127–133. https://doi.org/10.1140/epjb/e2007-00209-1.
[18] Wang Y L, Cui H L, Yu B R, et al. First-principle calculations of elastic properties of Wurtzite-type aluminum nitride under pressure. Commun. Theor. Phys., 2008, 49(2): 489. https://doi.org/10.1088/0253-6102/49/2/50.